Chemical Engineering Journal 444 (2022) 136458

Contents lists available at ScienceDirect

Chemical Engineering Journal

journal homepage: www.elsevier.com/locate/cej

Response of aerobic granular sludge to loading shock: Performance and proteomic study

Mingyue Geng [a], Shijie You [a], Haijuan Guo [b,*], Fang Ma [a,*], Xiao Xiao [a], Jinna Zhang [a], Xiping Ma [b]

[a] State Key Laboratory of Urban Water Resource and Environment, School of Environment, Harbin Institute of Technology, Harbin 150090, PR China
[b] School of Environment, Liaoning University, Shenyang 110036, PR China

ARTICLE INFO

Keywords:
Response mechanism
OLR shock
Aerobic granules
Sludge property
Proteomics

ABSTRACT

In this work, the response of aerobic granular sludge (AGS) to organic loading rate (OLR) shock was investigated from proteomic level for the first time. Results showed that OLR shock destabilized AGS system in terms of sludge properties, nutrient removal and microbial community, while they reached a new stability eventually. The AGS system exhibited larger-size granules (4 mm), higher biomass retention (6.9 g/L), enhanced nitrogen removal (97%-99%) and abundant *Candidatus_Competibacter* (30.7%) under OLR shock. Proteomic analysis demonstrated that AGS system responded to OLR shock by activating protection mechanism through up-regulating numerous metabolic pathways related to amino acid synthesis, aminoacyl-tRNA biosynthesis and gluconeogenesis. With the extension of OLR-shocking tests, AGS up-regulated metabolic pathways associated with glycogen synthesis and denitrification, which were mainly contributed by *Candidatus_Competibacter* based on species annotation analysis. This study offers an in-depth mechanistic insight into response of AGS to OLR shock and relevant regulation mechanisms, which will provide fundamental information and important implications for practically relevant cases.

1. Introduction

Aerobic granules are microbial aggregates with compact structure, higher biomass retention, excellent settleability and reduced footprints compared with conventional activated sludge [1,2]. These unique advantages make aerobic granular sludge (AGS) an advanced technology for biological wastewater treatment, and in the past few decades, the effectiveness of AGS has been demonstrated for treating a broad range of wastewater [3–6].

Organic loading rate (OLR) constitutes one of the key factors that exert influence on the formation and stability of AGS. In brief, low OLR usually results in the formation of small and compact granules and longer period for starting up the AGS system [7–9]. On the other hand, high OLR accelerates granulation of activated sludge and facilitates formation of granules with larger size, while less compact structure and poor stability of granules may be a concern [10–13]. A large number of studies focused on the boundary conditions of OLR for aerobic granulation and stability, showing the available OLR of 0.15–15 kg COD m^{-3} $d^{-1}$for successful granulation. For example, Chen et al. [8] successfully cultivated aerobic granular sludge with strong settleability and excellent nutrient removal under 0.15 kg COD m^{-3} d^{-1}. Long et al. [11] investigated the OLR tolerance of AGS in a cyclic aerobic granular reactor (CAGR) by increasing influent COD concentration, and results showed that AGS could withstand OLR up to 15 kg COD m^{-3} d^{-1}. The adaption in a wide range of OLRs and high tolerance to OLRs triggered AGS system adapt unfavorable conditions.

AGS system is known to present much greater resistance to OLR shock than activated sludge. However, most of studies mainly focused on macro-scale studies on OLR tolerance of AGS system, and little is known about the way how AGS system responded to OLR shock and how granular sludge regulated the mechanisms for resistance to OLR shock. From the viewpoint of engineered application, OLR may vary over a wide range for both domestic and industrial wastewater [14,15], and thus a particular importance needs to be emphasized to investigate the response and regulation of AGS system to OLR turbulence. This will be useful to further optimize the operational conditions of AGS system during practical application process.

Metaproteomics have been used successfully for identification of

* Corresponding authors..
E-mail addresses: guohaijuan@163.com (H. Guo), mafang@hit.edu.cn (F. Ma).

https://doi.org/10.1016/j.cej.2022.136458
Received 6 February 2022; Received in revised form 7 April 2022; Accepted 14 April 2022
Available online 18 April 2022

proteins in environmental samples on a quantitative basis, recording a remarkable applications directed toward biological wastewater treatment. By performing metaproteomics analysis, it was possible to identify the main proteins and elucidate relevant functions in enhanced biological phosphorus removal (EBPR) system [16]. Another example is reported by Azizan et al. [17] who interpreted the molecular mechanisms of poor ammonium removal in wastewater treatment system. However, to the best of our knowledge, it remains unclear for proteomic information in AGS system under OLR shock conditions. Protein expression is of particular importance because it offers a direct mechanistic reflection of microbial activities in ecosystems [18]. Performing proteomic analysis is expected to provide an in-depth proteomic-level insight into the underlying response and regulation mechanisms of AGS system when experiencing OLR shock.

The objectives of this study are to (i) investigate the response of AGS system to OLR shock in terms of physicochemical properties, nutrient removal and microbial community, (ii) analyze the protein expression of AGS system under OLR shock using label-free quantitative technique, (iii) elucidate the molecular response and regulation mechanisms under OLR shock. This study is expected to provide an in-depth insight into the response of AGS system to OLR shock from proteomic level, while offering fundamental information for the optimization of AGS technology in further engineering applications.

2. Materials and methods

2.1. Reactor operation

A sequencing batch reactor (SBR, 5 cm in diameter and 60 cm in height with a working volume of 1.2 L) was used in this work. The reactor was operated at 4-h operation cycle, comprising feeding (20 min), non aeration (40 min), aeration (170 min), settling (5 min) and decanting (5 min). The hydraulic retention time was 8 h. Air with a flow rate of 1.5 L/min was introduced from the bottom of reactor with fine bubble. The effluent was discharged from the middle of the reactor, resulting in a volumetric exchange ratio of 50%. The reactor was operated under OLR of 1.8 kg COD m^{-3} d^{-1} during 1–80 days and 3.6 kg COD m^{-3} d^{-1} during 81–160 days. To fulfill the objectives of this work, comparative analyses among different phases were opted (Table S1). The comparative analyses between phase I and phase II was to evaluate the response of AGS system to OLR shock. Comparison of phase II and phase III allowed to study the operation characteristics and stability of AGS system with the extension of OLR shock.

2.2. Inoculum and feeding

Stable granules developed at OLR of 1.8 kg COD m^{-3} d^{-1} were selected as inoculum in this work, whose culture strategy was described in previous study [19]. The granules for inoculum have maintained stable for more than 2 months with average particle size of 2 mm and SVI_{10} of 38 mL/g. Synthetic media fed to AGS system consisting of 60 mg/L ammonia nitrogen (NH_4^+-N), 10 mg/L total phosphorus (TP), 20 mg/L Mg^{2+}, 20 mg/L Fe^{2+}, 20 mg/L Ca^{2+} and 1 mL/L microelements. The detailed composition of trace element solution is listed in Table S2. Carbon source was provided by CH_3COONa, which increased from 600 mg COD/L to 1200 mg COD/L, corresponding to a OLR of 1.8 kg COD m^{-3} d^{-1} and 3.6 kg COD m^{-3} d^{-1}, respectively.

2.3. Microbial community analysis

The sludge samples for microbial community analysis were collected at phase I (denoted as S11), phase II (S22) and phase III (S33) during aeration mixing stage. The bacterial DNA from all the samples was extracted using E.Z.N.A.® soil DNA Kit (Omega Bio-tek, Norcross, GA, U.S.). 338F (5′-ACTCCTACGGGAGGCAGCAG-3′) and 806R (5′-GGACTACHVGGGTWTCTAAT-3′) were used as primers to amplify the V3-V4 hypervariable region of the 16S rRNA gene by thermocycler PCR system (GeneAmp 9700, ABI, USA). Sequencing of PCR products was performed on an Illumina MiSeq platform (Illumina, San Diego, USA).

2.4. Protein analysis using label-free quantitative technique

The sludge samples for proteomic analysis were collected at phase I, phase II and phase III during aeration mixing stage. Three biological replicates were used for each sludge sample. Proteins from the sludge samples were identified and analyzed using label-free quantitative technique proteomics. In brief, the procedures of label-free quantitative proteomics included protein extraction, protein quantification using Pierce™ BCA Protein Assay Kit, sodium dodecyl sulfate (SDS) - polyacrylamide gel electrophoresis (PAGE), reduction/alkylation, protease digestion by trypsin, peptides quantification and LC-MS/MS analysis. The details were described in the Supporting Information (Text S1).

2.5. Other analytical methods

COD, NH_4^+-N, nitrite nitrogen (NO_2^--N), nitrate nitrogen (NO_3^--N), total nitrogen (TN) concentrations of effluent and influent samples, as well as the mixed liquor suspended solids (MLSS), sludge volume index (SVI) of sludge samples were measured according to the standard methods [20]. Sludge retention time (SRT, day) and observed biomass yield (Y_{obs}, $gCOD_x/gCOD_{rem}$) were calculated according to previous studies (Text S2) [21–24]. The SRT in this study was approximately 20 ± 2 days. Particle size distribution and sludge mean size were measured using sieving methods [25]. Excellular protein and polysaccharides were extracted according to previous study [26]. Excellular protein and polysaccharides were quantified by Lowery method [27] and phenol–sulfuric acid method [28], respectively.

3. Results and discussion

3.1. Response of granular sludge to OLR shock

Fig. 1 shows the variation of sludge properties during the whole phase of operation. The AGS system under 1.8 kg COD m^{-3} d^{-1} (phase I, day 0–80) exhibited stable sludge properties with MLSS of 4.5 g/L, particle size of 2 mm and SVI_{10} of 37 mL/g (Fig. 1). To investigate the response of AGS system to OLR shock, OLR was increased from 1.8 kg COD m^{-3} d^{-1} to 3.6 kg COD m^{-3} d^{-1} on day 80. As a result, the sludge properties underwent significant change on day 80–100, followed by gradually reaching a new stability on day 101–160 under OLR shock (Fig. 1). In order to elucidate this response process clearly, we discussed the data by separating the two phases for OLR of 3.6 kg COD m^{-3} d^{-1} to phase II (day 80–100; variable phase) and phase III (day 101–160; stable phase). Furthermore, in order to ensure the significant change of AGS system with respect to OLR variation was the responses of AGS to OLR shock, rather than it was caused by the increase of running time, a control reactor with OLR of 1.8 kg COD m^{-3} d^{-1} was performed during the whole operational process. Stable AGS with an average particle size of 2 mm and biomass concentration of 4.5 g/L during 160-day operation further confirmed the response process of AGS system to OLR shock (Fig. S1). As shown in Fig. 1, both MLSS and SVI_{10} sharply increased (phase II) and then gradually stabilized at 6.5–6.9 g/L and 44–45 mL/g (phase III) under 3.6 kg COD m^{-3} d^{-1}, which were higher than 4.2–4.5 g/L and 36–38 mL/g under 1.8 kg COD m^{-3} d^{-1}, respectively. When OLR was increased from 1.8 kg COD m^{-3} d^{-1} to 3.6 kg COD m^{-3} d^{-1}, the observed biomass yield (Y_{obs}) value was increased from 0.14 $gCOD_x/gCOD_{rem}$ (phase I) to 0.22 $gCOD_x/gCOD_{rem}$ (Phase II) (Fig. S2). Liu and Tay [21] reported that the Y_{obs} obtained in AGS system was increased from 0.063 gVSS/gCOD to 0.137 gVSS/gCOD when OLR increased from 1.5 kg COD m^{-3} d^{-1} to 3 kg COD m^{-3} d^{-1}. Higher Y_{obs} means more excessive sludge production, most likely due to incomplete anaerobic internal storage of substrates under high OLR leading to overgrowth of

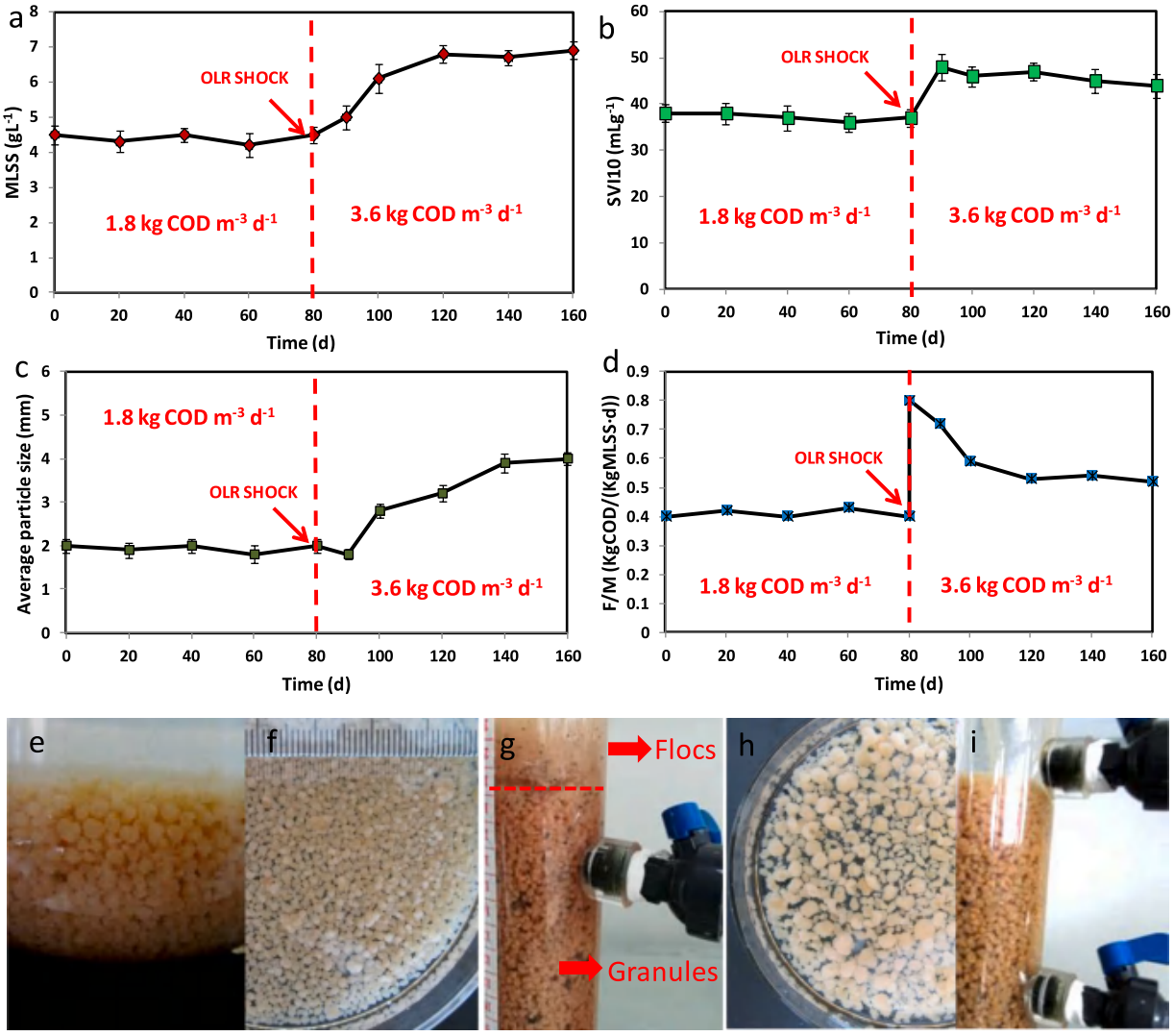

Fig. 1. Sludge properties (a-d) and morphology (e, f: phase I, g: phase II, h, i: phase III) during 160-day operation.

fast-growing microorganisms [29]. With the extension of operational time, Y_{obs} was decreased to 0.17 $gCOD_x/gCOD_{rem}$ at phase III (Fig. S2). Decreased biomass yield per COD_{rem} under 3.6 kg COD m^{-3} d^{-1} should result from the enriched polymer-storage microorganisms. This was consistent with previous studies where polymer-storage microorganisms such as glycogen accumulating organisms could convert substrates to polymers under anaerobic condition and grow on the stored polymers at a lower growth rate during aerobic period [29,30]. Average particle size decreased slightly first and then increased rapidly (phase II), stabilizing at approximately 4 mm eventually (phase III), the value being much higher than 2 mm under 1.8 kg COD m^{-3} d^{-1} (Fig. 1). Particle size distribution analysis demonstrated that the proportion of 4–6 mm granules increased to 50–60%, and the proportion of granules with 1–2 mm decreased to 9–12% under OLR shock (Fig. S3). These results indicated that AGS system under OLR shock exhibited high biomass concentration, large-sized granules and poor sludge settleability (day 80–160). Besides that, OLR shock stimulated a transient accumulation of flocculent sludge in AGS system. As shown in Fig. 1e-i, no visible flocs was observed during day 0–80 (Fig. 1e, f), while obvious flocs appeared on the upper layer of sludge bed during 80–100 days (Fig. 1g). Afterwards (day 101–160), they gradually disappeared and negligible flocculent sludge was observed on the upper layer of sludge bed (Fig. 1h, i). The short-lived flocs could also be confirmed and proved by the results of particle size distribution (Fig. S3). Clearly, the proportions of flocs (<200 μm) was stabilized at 3–6% under 1.8 kg COD m^{-3} d^{-1} (day 0–80), while it sharply increased to 15% (day 90) and then gradually recovered to approxiamtely 3% under 3.6 kg COD m^{-3} d^{-1} (Fig. S3). The changes of sludge properties may be attributed to the high food/microorganisms (F/M) ratio (Fig. 1d). Sudden increase of OLR from 1.8 kg COD m^{-3} d^{-1} to 3.6 kg COD m^{-3} d^{-1} resulted in a 2-fold increase in F/M value from 0.4 to 0.8 on day 80. High F/M was reported to increase sludge hydrophilicity, and thereby poor sludge settleability [31]. Furthermore, high F/M promoted rapid growth of microorganisms, which was not conducive to cell aggregation and facilitated the production of flocs [31,32]. Similarly, Hamza et al. [33] reported that rapid bacterial growth would out-compete biomass aggregation, resulting in the presence of flocs in AGS system. In this study, the flocs gradually disappeared along with reactor operation based on the results of sludge morphology and particle size distribution (Fig. 1h-i, Fig. 3S). The most likely reasons for the disappearance of flocs might be that (i) some flocs attached onto the surface of granules and poor settling flocs was washed out under short settling time (5 min) along with the operation [34–36]; (ii) the increased biomass concentration under high F/M ratio in turn decreased F/M ratio (Fig. 1d), slowing down the rate of microbial growth and thus contributing to the disappearance of flocs [32,33]; (iii) most COD was stored anaerobically by polymer-storage microorganims,

resulting in little available COD during aerobic period for fast-growing microorganism growth [29].

3.2. Nutrient removal by AGS under OLR shock

COD removal efficiency was shown to be stabilized at 92–94% during phase I (OLR of 1.8 kg COD m^{-3} d^{-1}, Fig. 2a). Increasing OLR from 1.8 kg COD m^{-3} d^{-1} to 3.6 kg COD m^{-3} d^{-1} led to a decrease in COD removal efficiency to 77% (phase II, Fig. 2a). The instant increase in influent COD offered excessive substrate than the biomass can be consumed, and thus the surplus substrate was observed in the effluent [37]. At phase III, COD removal efficiency was stabilized and recovered to higher than 90%. These results implied that OLR shock disturbed the stability of COD removal, while it was recovered to the initial level of 90% with good stability along with the operation. Cyclic test of AGS performance at phase III suggested that majority of influent COD was removed during the first 60-min non-aeration period, accounting for COD concentration lower than 50 mg/L from the 80th min to the end of aeration period (Fig. S4a). In other words, the microorganisms at phase III were likely to sustain at starvation stage during aeration period. In comparison, higher effluent COD concentration (270 mg/L) at phase II suggested sufficient carbon source available for growth of microorganisms during the whole operational cycle. It was known that the feeding substrates were utilized for microbial growth and stored as intracellular polymers under anaerobic condition [30,38]. Thus, high biomass concentration at phase III resulted in greater capability for COD removal under anaerobic period compared with phase II, which should be responsible for high COD removal during non-aeration period (Fig. S4a).

As shown in Fig. 2b, TN removal efficiency was stabilized at 52.5–71.9% during pahse I. When the OLR was increased from 1.8 kg COD m^{-3} d^{-1} to 3.6 kg COD m^{-3} d^{-1}, effluent NO_3^--N concentration was found to drop from 25.4 mg/L to 10.8 mg/L, corresponding to an increase in TN removal efficiency from approximately 56% to 80% at phase II (Fig. 2b). This result was not surprising as OLR shock along with excessive exogenous carbon source promoted nitrogen removal at phase II in AGS system (Fig. 2a). At phase III, TN removal was further improved to the efficiency of 97%-99% on day 145 until the end of operation, and the NO_3^--N and NO_2^--N concentration were<0.5 mg/L (Fig. 2b). This indicated excellent denitrification performance of AGS system. This confirmed that the OLR shock disturbed the stability of nitrogen removal, while extending OLR shock could stabilize higher nitrogen removal. The enhanced TN removal and lower effluent NO_3^--N and NO_2^--N concentration at phase III than phase II should be attributed to larger-sized particles at phase III (Fig. 1). Compared with small particle size and floc presence at phase II, the larger-sized granules and full granulation at phase III created more anoxic space for growth of anerobe and facultative aerobe, which facilitated growth of functional microorganisms relevant to nitrogen removal [11,26]. NH_4^+-N removal efficiency reached a level being close to 100% during the whole phase of operation (data not shown). Cyclic tests at phase III indicated that the NH_4^+-N was mainly removed during 60–120 min aeration period (Fig. S4b). Moreover, slight decrease of NH_4^+-N concentration during 0–60 min was observed (Fig. S4b). The slight decrease of ammonia nitrogen concentration was likely due to microbial assimilation. Under sufficient carbon source condition, microbes would consume ammonia nitrogen to convert into cellular substances [39]. NO_3^--N concentration was maintained between 0.8 mg/L and 1.9 mg/L throughout the cyclic test with slight accumulation of NO_2^--N at 120 min (5.1 mg/L), followed by gradual decline to 0.2 mg/L at the end of test. This phenomenon might have connections with lower reduction rate of NO_2^--N than the reduction rate of NO_3^--N [40].

3.3. Analysis of microbial community under OLR shock

Microbial community was analyzed to investigate the response of AGS to OLR shock. PCoA analysis illustrated that the microbial community in AGS system changed significantly under OLR shock, which could also be confirmed by the stable microbial community in control reactor with OLR of 1.8 kg COD m^{-3} d^{-1} throughout the whole phase (Fig. S5). Microbial community composition at phylum suggested that *Proteobacteria*, *Bacteroidota* and *Chloroflexi* were the dominant phyla in all the samples collected from three phases of operation, accounting for 72.4%, 15.3% and 3.26% in S11 (phase I), 41.9%, 45.5% and 3.76% in S22 (phase II) and 66.1%, 20.5% and 7.32% in S33 (phase III), respectively (Fig. 3a). When the OLR was increased from 1.8 kg COD m^{-3} d^{-1} to 3.6 kg COD m^{-3} d^{-1}, there was an observation of sharp decline in *Proteobacteria* abundance from 72.4% to 41.9%, an increase in *Bacteroidota* abundance from 15.3% to 45.5% and *Chloroflexi* abundance from 3.26% to 3.76%. This indicated that the OLR shock facilitated the growth and enrichment of phyla *Bacteroidota* and *Chloroflexi*, driving the shift of most abundant bacteria from phyla *Proteobacteria* at phase I to *Bacteroidota* at phase II (Fig. 3a). With the extension of operational time, phyla *Proteobacteria* abundance was increased to the level becoming the most abundant one again. That is, the OLR shock could cause the shift of the most abundant phyla, but the shift could be recovered to the initial state along with the operation. In spite of this, the relative abundance of phyla *Proteobacteria* at phase III (66.1%) remained lower than that of phase I (72.4%), whereas the relative abundance of phyla *Bacteroidota* at phase III (20.5%) was higher than that of phase I (15.3%, Fig. 3a). Besides that, the relative abundance of phyla *Chloroflexi* at phase III was 7.32%, representing a value being 2.25 times higher than that of phase I (3.26%, Fig. 3a).

Fig. 3b reveals the composition of bacterial community under three phases at genus level. The dominant genera were *Paracoccus* (25.6%), norank_f_*Rhodobacteraceae* (21.5%) and *Microscillaceae* OLB12 (10.6%) in S11, norank_f_*Saprospiraceae* (13.1%), *Microscillaceae* OLB12 (11.9%), *Flavobacterium* (9.89%) and *Thauera* (6.10%) in S22, *Candidatus_Competibacter* (30.7%) and *Flavobacterium* (10.6%) in S33. When

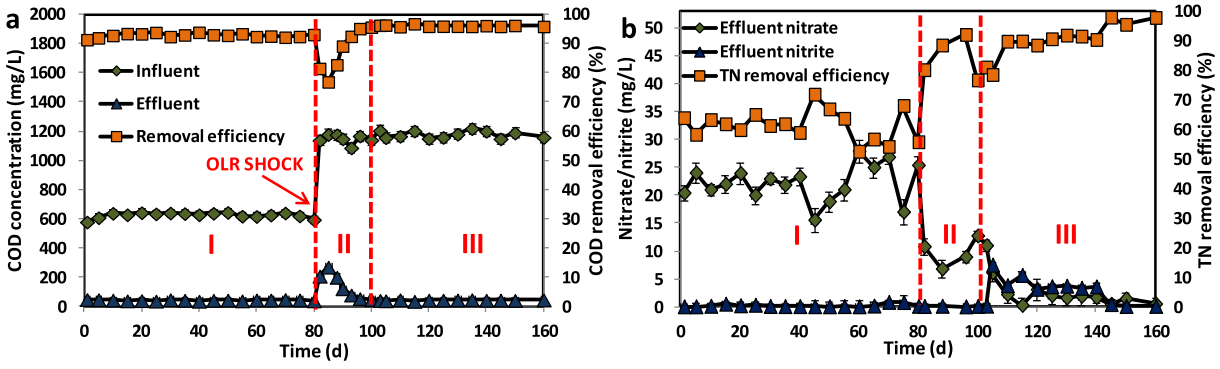

Fig. 2. Profiles of COD (a) and nitrogen (NO_3^--N, NO_2^--N, TN) (b) during the whole operation.

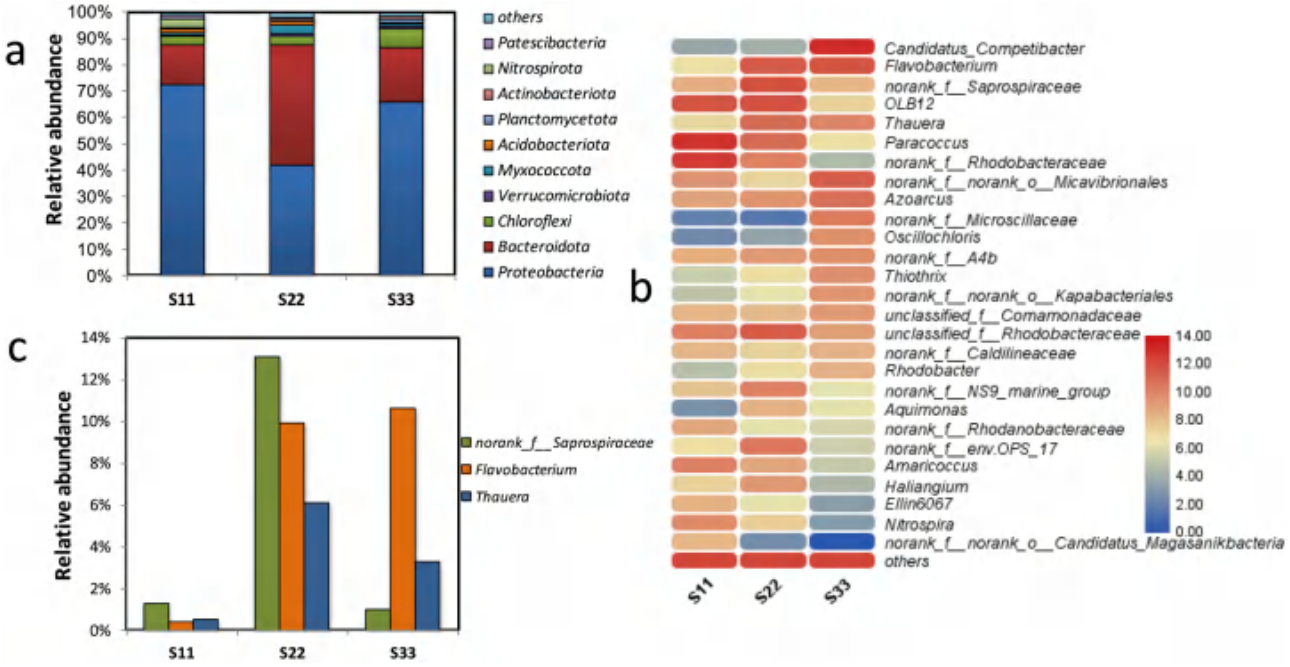

Fig. 3. Bacterial community composition of S11, S22 and S33 at phylum (a) and genus level (b), the variations of norank_f_*saprospiraceae*, *flavobacterium* and *thauera* at different phases (c).

the OLR was increased from 1.8 kg COD m^{-3} d^{-1} to 3.6 kg COD m^{-3} d^{-1}, the relative abundance of *Microscillaceae* OLB12 remained relatively stable of approximately 11%, while that of norank_f_*Saprospiraceae*, *Flavobacterium* and *Thauera* was increased from 1.29%, 0.392% and 0.505% to 13.1%, 9.89% and 6.10%, respectively (Fig. 3b-c). This suggested the OLR shock to be beneficial for growth and enrichment of norank_f_*Saprospiraceae*, *Flavobacterium* and *Thauera*. Combined with the result of floc appearance at phase II (Fig. 1f), it was reasonable to infer that the flocs stimulated by OLR shock were mainly composed of norank_f_*Saprospiraceae*, *Flavobacterium* and *Thauera*. At phase III, the relative abundance of norank_f_*Saprospiraceae* was decreased significantly from 13.1% to 1.00%, and that of *Thauera* was decreased from 6.10% to 3.28% (Fig. 3c). On the contrary, the *Flavobacterium* abundance altered slightly, *i. e.* valued 10% by the end of operation (Fig. 3b-c). These results indicated that most norank_f_*Saprospiraceae* was washed out, while *Flavobacterium* and part of *Thauera* were retained in the reactor. The decrease in norank_f_*Saprospiraceae* and *Thauera* was likely due to washout of poor-settling flocs under short settling time. In addition, the relative abundance of *Candidatus_Competibacter* was increased sharply to 30.7%, which became the most dominant genera under OLR shock. The *Candidatus_Competibacter* was known as slow-growing carbon-storing organisms capable of converting readily degradable substrates to intracellular storage polymers under anaerobic condition [30,41]. Thus, the abundant *Candidatus_Competibacter* should be responsible for the high COD removal in non-aeration period under OLR shock (Fig. S4a). During the aeration period at phase III where microorganisms were in starvation (Fig. S4a), the abundant *Candidatus_Competibacter* was capable of consuming storage polymers for supporting growth with nitrate/nitrite serving as electron acceptor, which was consistent with the enhanced nitrogen removal at phase III (Fig. 2, S4b). In addition, the abundance of some denitrifying bacteria such as *Thauera* decreased at phase III compared with phase II (Fig. 3), this result further suggested that the sharp increased *Candidatus_Competibacter* played important roles in the enhanced nitrogen removal at phase III (Figs. 2 and 3). Compared with phase I, OLR shock increased the influent COD concentration and supplied more carbon source at non-aeration phase. Higher COD concentration means higher driving force for transportation of substrate from bulk liquid to granule interior. Both two factors created a favorable condition for growth and enrichment of *Candidatus_Competibacter* [30,42].

3.4. Response mechanism of AGS to OLR shock from protein level

We studied and confirmed that AGS made responses to resist OLR stress and eventually reached a new stability along with the operation. In order to underline the way AGS responded to OLR shock and AGS regulated the mechanisms for resisting OLR shock at protein level, label-free quantitative technique was used to analyze the differently expressed proteins (DEPs) and corresponding metabolic pathways among different phases. In this study, the differences of proteomic information in AGS system before (day 0–80) and after (day 80–160) OLR shock was discussed.

3.4.1. Protein expression of AGS to OLR shock

In this study, differentially expressed proteins (DEPs) in "S22 vs S11" and "S33 vs S22" groups were analyzed. The DEPs were selected based on $p < 0.05$, down-regulation FC < 0.5 and up-regulation FC > 2. Gene Ontology (GO) is a description of gene function based on a comprehensive database [43,44]. According to GO annotation, genes and gene products can be classified into molecular function (MF), cellular component (CC), and biological process (BP) [45,46]. As shown in Fig. 4, the DEPs in "S22 vs S11" and "S33 vs S22" groups were annotated according to Gene Ontology (GO), providing an overview of the DEPs based on their functions.

Molecular function analysis revealed that most of DEPs were related to catalytic activity and binding activity in both "S22 vs S11" and "S33 vs S22" groups (Fig. 4a). Since catalytic activity is associated with enzymes involved in biochemical reactions, a large amount of DEPs responsible for catalytic activity indicated significant change of cell activity induced by OLR shock [47]. Furthermore, analysis for subgroups of catalytic activity revealed transferase activity, oxidoreductase activity and hydrolase activity to be the main catalytic activity in both "S22 vs S11" and "S33 vs S22" groups (Fig. S6a-b). For "S22 vs S11" group, more up-regulated proteins were observed in relation to transferase activity and oxidoreductase activity than down-regulated proteins, while fewer up-regulated proteins associated with hydrolase

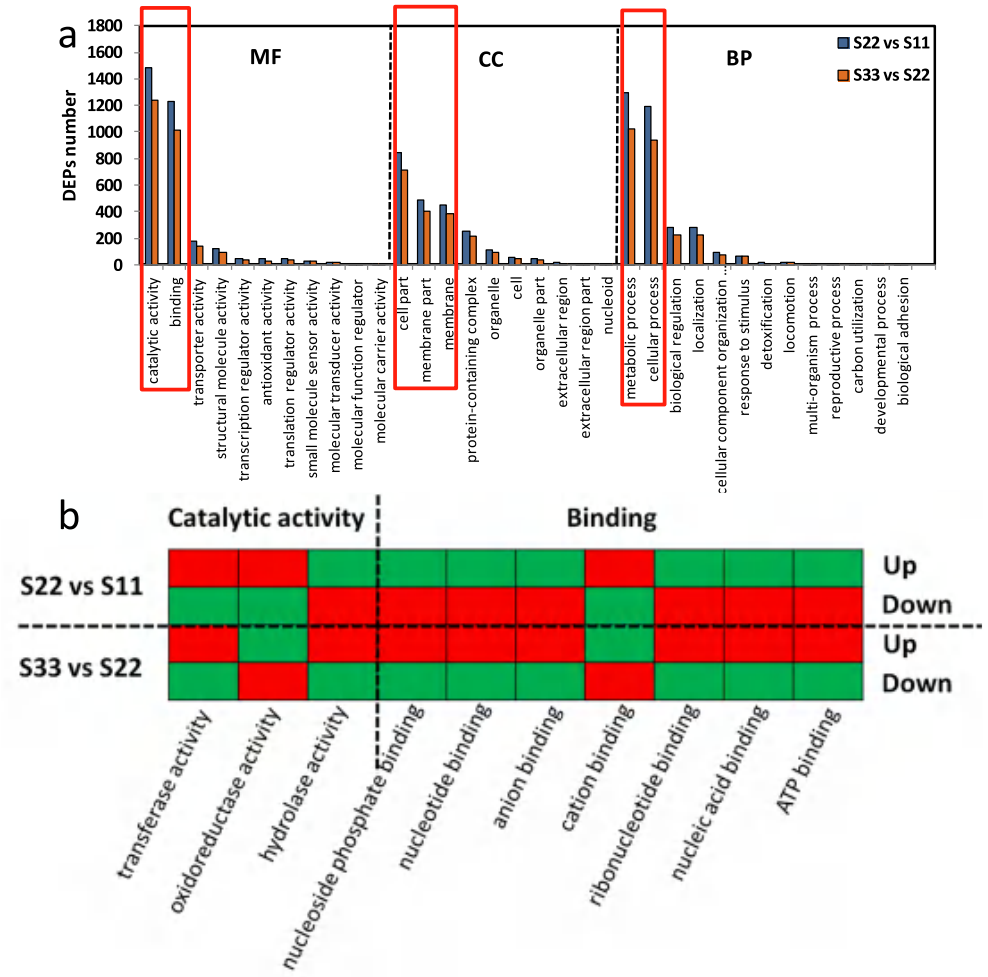

Fig. 4. The classification of DEPs in "S22 vs S11" and "S33 vs S22" groups based on Gene Ontology (GO) secondary level (a), comparison of the up- and down-regulated proteins associated with catalytic activity and binding in "S22 vs S11" and "S33 vs S22" groups (b). Note: the red color means up-regulated (down-regulated) proteins were more than down-regulated (up-regulated) proteins, and green color means up-regulated (down-regulated) proteins were fewer than down-regulated (up-regulated) proteins.

activity than down-regulated proteins (Fig. 4b). In comparison, the up-regulated proteins relevant to transferase activity and hydrolase activity were more than down-regulated proteins, while fewer up-regulated proteins associated with oxidoreductase activity than down-regulated proteins in "S33 vs S22" group (Fig. 4b). These results demonstrated that the expression of transferase activity proteins was always enhanced during the whole phase of operation. This suggested an essential role of transferase activity proteins in AGS system under OLR shock. Besides that, the expression of oxidoreductase activity and hydrolase activity proteins behaved differently between "S22 vs S11" and "S33 vs S22" groups (Fig. 4b). At phase II, sudden increase in COD concentration led to excessive exogenous substrates fed into reactor, and thus up-regulated oxidation–reduction reactions. At phase III, microorganisms contained within granules experienced starvation under low exogenous carbon source (Fig. S4a). As a result, they were forced to hydrolyze macromolecular substances to obtain sufficient carbon and energy source available for cell growth [48], and thus up-regulated the expression of proteins associated with hydrolase activity.

In addition, high fraction of DEPs relevant to binding activity in both "S22 vs S11" and "S33 vs S22" groups implied a significant change of binding activity proteins in AGS system under OLR shock (Fig. 4a). The function of binding is associated with the selective binding interaction between relevant molecules [47]. Analysis for subgroups of binding activity showed the nucleoside phosphate, nucleotide, cation, anion, nucleic acid, ribonucleotide and ATP binding to be the dominant binding functions of DEPs in "S22 vs S11" and "S33 vs S22" groups (Fig. S6c-d). In "S22 vs S11" gourp, OLR shock presented inhibition on the expression of binding proteins mentioned above except for the proteins with cation binding function. On the contrary, most binding proteins except for cation binding proteins were enhanced in "S33 vs S22" group (Fig. 4b). Considering more abundant cation binding proteins in suspended sludge rather than biofilm [47], this may provide the most likely explanation to higher amount of cation binding proteins in "S22 vs S11" group with the presence of flocs at phase II. On the other hand, cell aggregation was adversely impacted by declined cell hydrophobicity due to the presence of amino groups in anion-binding proteins [43,49]. The down-regulation of anion binding proteins in "S22 vs S11" group implied the improvement of microbial aggregation to withstand OLR shock in AGS system. Nevertheless, the SVI_{10} at phase II was higher than that of phase I, probably due to the presence of flocs at phase II (Fig. 1f). The increase of OLR from 1.8 kg COD m^{-3} d^{-1} to 3.6 kg COD m^{-3} d^{-1} resulted in a sudden and sharp increase of F/M and thus fast biomass growth. The high microbial growth rate could exceed the aggregation capacity of microorganisms and resulted in floc appearance (Fig. 1f) [33]. Thus, the presence of poorsettling flocs in reactor increased the SVI_{10} at phase II. Furthermore, with the extension of operational time, improved expression of anion binding protein suggested negative impact of long-term OLR shock on sludge aggregation. This appeared to be in good agreement with previous studies where high OLR facilitated sludge aggregation and rapid aerobic granulation while the resulting granules were loosely structured and unstable with the extension of operational time [12,13].

With regard to cell component and biological process, a large number of DEPs in both "S22 vs S11" and "S33 vs S22" groups located in cell

part and participated in metabolic and cellular processes (Fig. 4a). Besides that, the amount of up-regulated proteins were more than down-regulated proteins in both "S22 vs S11" and "S33 vs S22" groups (Fig. S7), implying that OLR shock promoted the expression of proteins located in cell part and involved in metabolic and cellular process.

3.4.2. Metabolic pathway of AGS to OLR shock

To gain further insights into the response mechanisms of AGS to OLR shock from protein level, the analysis and discussion of metabolic pathways were necessary. In this study, the Kyoto Encyclopedia of Genes and Genomes (KEGG) pathway enrichment of up-regulated proteins identified in "S22 vs S11" and "S33 vs S22" groups was analyzed. Fig. 5 shows the overview of KEGG pathway significantly enriched in "S22 vs S11" and "S33 vs S22" groups ($p < 0.05$). Clearly visible is that the OLR shock exhibited a significant impact on the metabolic pathways. Fig. 5a-b illustrated 35 pathways enriched in "S22 vs S11" group and 24 pathways in "S33 vs S22" group, respectively. Among these enriched pathways, 10 pathways were found to be shared by "S22 vs S11" and "S33 vs S22" groups, whereas 25 pathways were unique in "S22 vs S11" group and 14 unique pathways in "S33 vs S22" group (Fig. 5c). This suggested 10 shared pathways to be up-regulated during the whole operation. The 10 shared pathways might have contribution as essential pathways for facilitating AGS system to resist OLR shock and recover stability. As shown in Fig. 5d, 10 shared pathways were identified to consist of carbon metabolism (ko01200), biosynthesis of amino acids (ko01230), cirtate cycle (TCA cycle, ko00020), propanoate metabolism (ko00640), glycolysis/gluconeogenesis (ko00010), quorum sensing (ko02024), alanine, aspartate and glutamate metabolism (ko00250), arginine biosynthesis (ko00220), degradation of aromatic compounds (ko01220) and biofilm formation-pseudomonas aeruginosa (ko02025).

Primary metabolic pathways, *i. e.* biosynthesis of amino acids, carbon metabolism, glyconegenesis, and TCA cycle, were up-regulated in both "S22 vs S11" and "S33 vs S22" groups, suggesting OLR shock to activate TCA cycle and stimulate amino acids and glucose synthesis through central carbon metaoblism. In "S22 vs S11" group, numerous pathways associated with amino acid metabolism were up-regulated, which included valine, leucine and isoleucine biosynthesis (ko00290), lysine biosynthesis (ko003000), phenylalanine, tyrosine and tryptophan biosynthesis (ko00400), arginine biosynthesis (ko00220), alanine, aspartate and glutamate metabolism (ko00250), cysteine and methionine metabolism (ko00270), glycine, serine and threonine metabolism (ko00260), phenylalanine metabolism (ko00360), tryptophan metabolism (ko00380), histidine metabolism (ko00340), lysine degradation (ko00310) (Fig. 6a). Details of these pathways showed that 18 kinds of amino acid synthesis pathways were up-regulated in "S22 vs S11" group, including cysteine (cys), methionine (met), glycine (gly), threonine (thr), alanine (ala), aspartate (asp), asparagine (asn), glutamate (glu), glutamine (gln), valine (val), isoleucine (ile), leucine (leu), arginine (arg), tryptophan (trp), phenylalanine (phe), tyrosine (tyr), lysine (lys), histidine (his) (Fig. 6c). Based on these results, the AGS system was likely to up-regulate amino acid synthesis pathways in response to OLR shock, which might help AGS system to resist the OLR stress. Most of amino acids except val, lys and arg were considered indispensable for extracellular protein (PN) [50,51]. Combined with the significantly up-

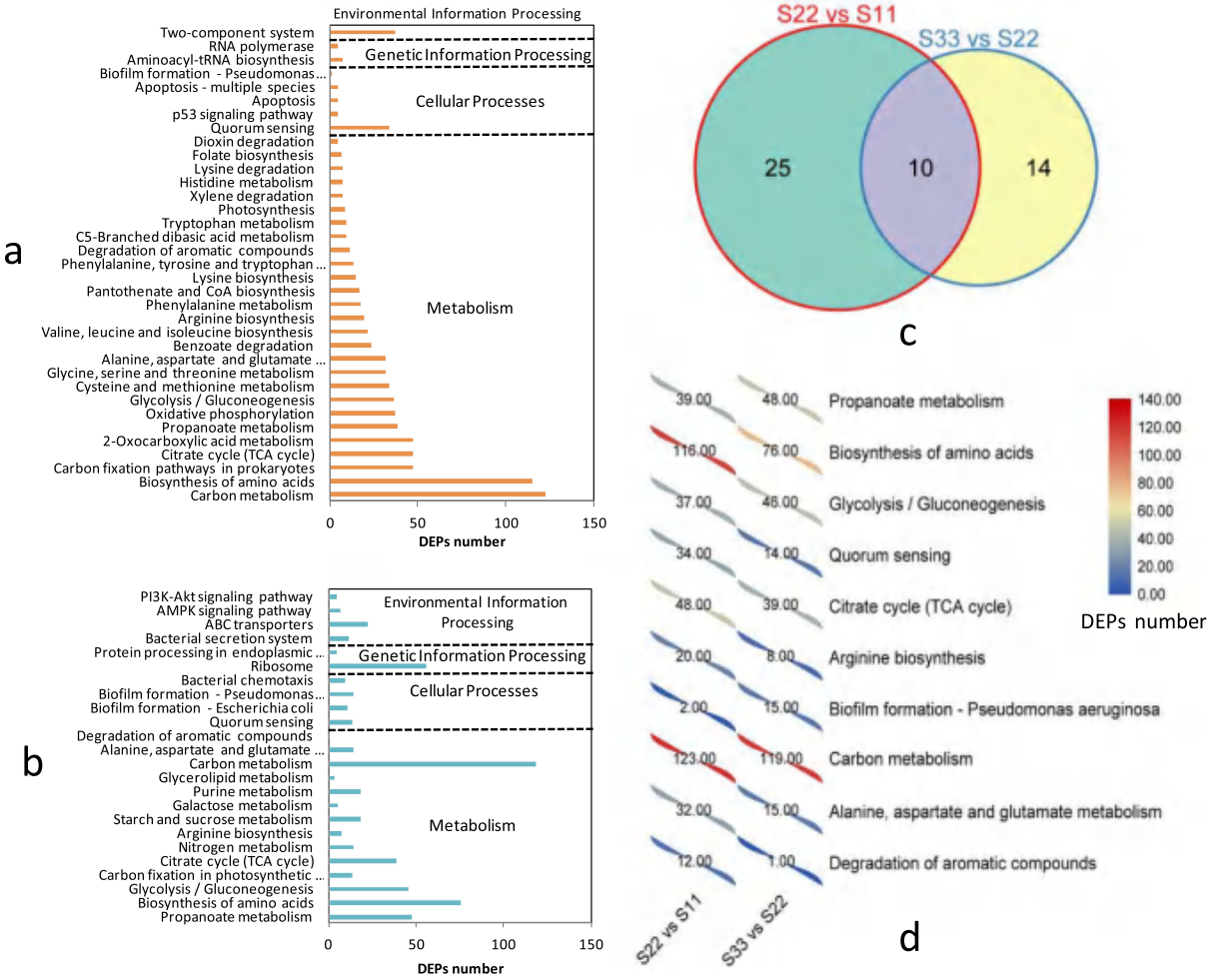

Fig. 5. KEGG pathway analyses of the up-regulated proteins in "S22 vs S11" and "S33 vs S22" groups.

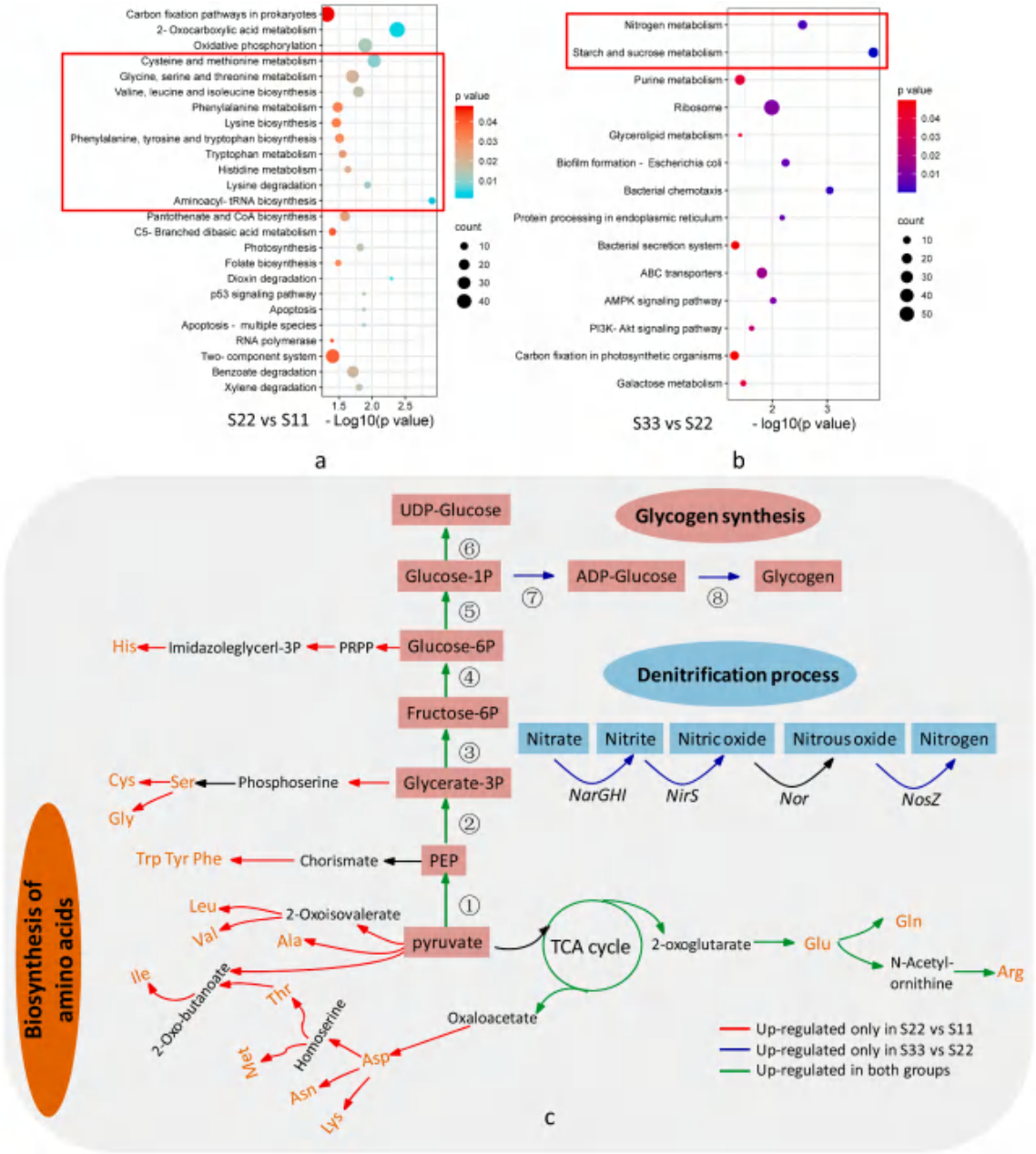

Fig. 6. The KEGG pathways significantly enriched only in "S22 vs S11" (a) and "S33 vs S22" (b) groups ($p < 0.05$), the network of amino acid synthesis, glycogen synthesis and denitrification pathways (c).

regulated aminoacyl-tRNA biosynthesis pathway in "S22 vs S11" group (Fig. 6a), PN synthesis could be activated at phase II. This result is consistent with the enhanced PN production under OLR shock (Fig. S8). Similar results were obtained by Paulo. et al [52], who found most of the bacteria within granules were excellular polymeric substance producers during higher OLR period. A function frequently attributed to extracellular polymeric substances was their protective effect in microorganisms against stressful environments [52–55]. Thus, AGS system was able to synthesize more amino acids closely related to excellular polymeric substances to protect it from turbulent influent COD concentration and OLR shock. By contrast, only 2 pathways (ko00250, ko00220) related to amino acid metabolism and corresponding 3 kinds of amino acid (glu, gln, arg) synthesis were up-regulated in "S33 vs S22" group, a value being much fewer than 11 pathways in "S22 vs S11" group (Fig. 6). These results suggested that the AGS system could activate a protection mechanism through upregulating a large number of amino acid synthesis pathways in response to influent COD turbulence. Furthermore, gluconeogenesis pathway was up-regulated in both "S22 vs S11" and "S33 vs S22", in which uridine diphosphate glucose (UDP-glucose) synthesis was up-regulated (Fig. 6). It is known that the basic pathway of polysaccharides (PS) synthesis played a determinstic role in the PS content in excellular polymeric substances [51]. The up-regulated UDP-glucose in "S22 vs S11" group was consistent with the activated excellular polymeric substances protection mechanism in response to OLR shock. In "S33 vs S22" group, glycogen synthesis pathway was remarkably up-regulated (Fig. 6). To further analyze the enzyme involved in glycogen synthesis process in "S33 vs S22" group, species annotation analysis of the up-regulated proteins related to glycogen synthesis according to NR database was carried out (Table S3). Results showed that most of the up-regulated proteins during glycogen synthesis process (13/19) in "S33 vs S22" group were originated from *Candidatus_Competibacter* (Table S3). Additionally, the nitrogen metabolism in

"S33 vs S22" group was up-regulated (Fig. 6b). As shown in Fig. 6c, the expression of *narGHI*, *nirS* and *nosZ* was remarkably up-regulated. It was known that *NarGHI*, *nirS* and *nosZ* were key enzymes involved in denitrification. The up-regulation of *narGHI*, *nirS* and *nosZ* was in line with the enhanced nitrogen removal at phase III (Fig. 2b). In addtion, species annotation suggested that most of the enzymes (4/6) involved in denitrification were originated from *Candidatus_Competibacter* (Table S4). The *Candidatus_Competibacter* was reported to consume intracellular storage polymer substrates for carbon source in famine phase, resulting in synthesis of glycogen through gluconeogenesis pathway and generating electron equivalents [30,56]. Although OLR shock caused excessive substrates at phase II, the soluble acetate was almost removed during the first 60-min non-aeration period at phase III, and this allowed a low substrate concentration in aeration stage (Fig. S4a). As a result, microorganisms within granules were unlikely to gain enough nutrient and energy sources from bulk liquid, and thus alternatively consumed intracellular substrates for survival. The large-sized particles created anoxic zone for microorganisms within granules (Fig. 1). In anoxic micro-environment, nitrate/nitrite could be utilized as electron acceptor for the intracellular carbon oxidation within *Candidatus_Competibacter*, resulting in up-regulated denitrification process in "S33 vs S22" group.

4. Conclusions

OLR shock disturbed the stability of AGS system in terms of sludge properties, nutrient removal and microbial community, while they reached a new stability eventually along with the operation. From proteomic level, AGS system responded OLR shock by up-regulating numerous metabolic pathways in relevance to amino acid synthesis, aminoacyl-tRNA biosynthesis and gluconeogenesis. With the extension of operational time, AGS system up-regulated metabolic pathways associated with glycogen synthesis pathway and denitrification, which was attributed to *Candidatus_Competibacter* based on species annotation analysis.

Declaration of Competing Interest

The authors declare that they have no known competing financial interests or personal relationships that could have appeared to influence the work reported in this paper.

Acknowledgement

This work was supported by the National Natural Science Foundation of China (Nos. 51878237 and 52070054). We would also like to acknowledge the assistance of HIT Yixing Academy of Environmental Protection and Heilongjiang Touyan Team.

Appendix A. Supplementary data

Supplementary data to this article can be found online at https://doi.org/10.1016/j.cej.2022.136458.

References

[1] M. Pronk, M.K. de Kreuk, B. de Bruin, P. Kamminga, R. Kleerebezem, M.C.M. van Loosdrecht, Full scale performance of the aerobic granular sludge process for sewage treatment, Water Res. 84 (2015) 207–217, https://doi.org/10.1016/j.watres.2015.07.011.

[2] S.S. Adav, D.J. Lee, K.Y. Show, J.H. Tay, Aerobic granular sludge: recent advances, Biotechnol. Adv. 26 (2008) 411–423, https://doi.org/10.1016/j.biotechadv.2008.05.002.

[3] C. Ramos, M.E. Suárez-Ojeda, J. Carrera, Long-term impact of salinity on the performance and microbial population of an aerobic granular reactor treating a high-strength aromatic wastewater, Bioresour. Technol. 198 (2015) 844–851, https://doi.org/10.1016/j.biortech.2015.09.084.

[4] S.J. Sarma, J.-H. Tay, Carbon, nitrogen and phosphorus removal mechanisms of aerobic granules, Crit. Rev. Biotechnol. 38 (2018) 1077–1088, https://doi.org/10.1080/07388551.2018.1451481.

[5] H. Wang, Q. Song, J. Wang, H. Zhang, Q. He, W. Zhang, J. Song, J. Zhou, H. Li, Simultaneous nitrification, denitrification and phosphorus removal in an aerobic granular sludge sequencing batch reactor with high dissolved oxygen: effects of carbon to nitrogen ratios, Sci. Total Environ. 642 (2018) 1145–1152, https://doi.org/10.1016/j.scitotenv.2018.06.081.

[6] Q. He, L. Chen, S. Zhang, R. Chen, H. Wang, Hydrodynamic shear force shaped the microbial community and function in the aerobic granular sequencing batch reactors for low carbon to nitrogen (C/N) municipal wastewater treatment, Bioresour. Technol. 271 (2019) 48–58, https://doi.org/10.1016/j.biortech.2018.09.102.

[7] J.-H. Tay, S. Pan, Y. He, S.-T.-L. Tay, Effect of organic loading rate on aerobic granulation. I: reactor performance, J Environ. Eng 130 (2004) 1094–1101, https://doi.org/10.1061/(ASCE)0733-9372(2004)130:10(1094).

[8] H. Chen, A. Li, C. Cui, F. Ma, D. Cui, H. Zhao, Q. Wang, B. Ni, J. Yang, AHL-mediated quorum sensing regulates the variations of microbial community and sludge properties of aerobic granular sludge under low organic loading, Environ Int. 130 (2019), 104946, https://doi.org/10.1016/j.envint.2019.104946.

[9] Y.Q. Liu, B.Y. Moy, J.H. Tay, COD removal and nitrification of low-strength domestic wastewater in aerobic granular sludge sequencing batch reactors, Enzyme Microb. Technol. 42 (2007) 23–28, https://doi.org/10.1016/j.enzmictec.2007.07.020.

[10] O.T. Iorhemen, Y. Liu, Effect of feeding strategy and organic loading rate on the formation and stability of aerobic granular sludge, J Water Process Eng. 39 (2021), 101709, https://doi.org/10.1016/j.jwpe.2020.101709.

[11] B. Long, C.-Z. Yang, W.-H. Pu, J.-K. Yang, F.-B. Liu, L. Zhang, J. Zhang, K. Cheng, Tolerance to organic loading rate by aerobic granular sludge in a cyclic aerobic granular reactor, Bioresour. Technol. 182 (2015) 314–322, https://doi.org/10.1016/j.biortech.2015.02.029.

[12] Y.-Q. Liu, J.-H. Tay, Fast formation of aerobic granules by combining strong hydraulic selection pressure with overstressed organic loading rate, Water Res. 80 (2015) 256–266, https://doi.org/10.1016/j.watres.2015.05.015.

[13] Y.-M. Zheng, H.-Q. Yu, S.-J. Liu, X.-Z. Liu, Formation and instability of aerobic granules under high organic loading conditions, Chemosphere 63 (2006) 1791–1800, https://doi.org/10.1016/j.chemosphere.2005.08.055.

[14] A.M.S. Paulo, C.L. Amorim, J. Costa, D.P. Mesquita, E.C. Ferreira, P.M.L. Castro, High carbon load in food processing industrial wastewater is a driver for metabolic competition in aerobic granular sludge, Front. Environ. Sci. 9 (2021) 388, https://doi.org/10.3389/fenvs.2021.735607.

[15] S.F. Corsino, D. Di Trapani, M. Torregrossa, G. Viviani, Daniele Di Trapani, Michele Torregrossa, Gaspare Viviani, Aerobic granular sludge treating high strength citrus wastewater: analysis of pH and organic loading rate effect on kinetics, performance and stability, J. Environ Manage. 214 (2018) 23–35, https://doi.org/10.1016/j.jenvman.2018.02.087.

[16] P. Wilmes, P.L. Bond, The application of two-dimensional polyacrylamide gel electrophoresis and downstream analyses to a mixed community of prokaryotic microorganisms, Environ. Microbiol. 6 (2004) 911–920, https://doi.org/10.1111/j.1462-2920.2004.00687.x.

[17] A. Azizan, F. Kaschani, H. Barinas, S. Blaskowski, M. Kaiser, M. Denecke, Using proteomics for an insight into the performance of activated sludge in a lab-scale WWTP, Int. Biodeterior. Biodegradation 149 (2020), 104934, https://doi.org/10.1016/j.ibiod.2020.104934.

[18] P. Wilmes, P.L. Bond, Towards exposure of elusive metabolic mixed-culture processes: the application of metaproteomic analyses to activated sludge, Water Sci. Technol. 54 (2006) 217–226, https://doi.org/10.2166/wst.2006.390.

[19] M. Geng, S. You, H. Guo, F. Ma, X. Xiao, J. Zhang, Impact of fungal pellets dosage on long-term stability of aerobic granular sludge, Bioresour. Technol. 332 (2021), 125106, https://doi.org/10.1016/j.biortech.2021.125106.

[20] Apha, Standard Methods for the Examination of Water and Wastewater Analysis, APHA-AWWA-WEF, Washington DC, 2005.

[21] Y.Q. Liu, J.H. Tay, Influence of cycle time on kinetic behaviors of steady-state aerobic granules in sequencing batch reactors, Enzyme Microb Technol. 41 (2007) 516–522, https://doi.org/10.1016/j.enzmictec.2007.04.005.

[22] Y.-Q. Liu, X. Zhang, R. Zhang, Wen-Tso Liu, J.-H. Tay, Effects of hydraulic retention time on aerobic granulation and granule growth kinetics at steady state with a fast start-up strategy, Appl. Microbiol. Biotechnol. 100 (2016) 469–477, https://doi.org/10.1007/s00253-015-6993-3.

[23] Y.-M. Liang, Y.-L. Yang, Y.-W. Chang, J.-Y. Chen, C.-W. Li, J.-H. Yu, S.-S. Chen, Shiao-ShingChen, comparison of high pressure and ambient pressure aerobic granulation sequential batch reactor processes, Bioresour. Technol. 140 (2013) 28–35, https://doi.org/10.1016/j.biortech.2013.04.042.

[24] B. Zhang, W.u. Lian, W. Shi, Zhiqiang Zhang, P.N.L. Lens, A novel strategy for rapid development of a self-sustaining symbiotic algal-bacterial granular sludge: applying algal-mycelial pellets as nuclei, Water Res. 214 (2022), 118210, https://doi.org/10.1016/j.watres.2022.118210.

[25] N. Derlon, J. Wagner, R.H.R. da Costa, E. Morgenroth, Formation of aerobic granules for the treatment of real and low-strength municipal wastewater using a sequencing batch reactor operated at constant volume, Water Res. 105 (2016) 341–350, https://doi.org/10.1016/j.watres.2016.09.007.

[26] M. Geng, F. Ma, H. Guo, D. Su, Enhanced aerobic sludge granulation in a sequencing batch reactor (SBR) by applying mycelial pellets, J. Clean. Prod. 274 (2020) 123037, https://doi.org/10.1016/j.jclepro.2020.123037.

[27] N. Bradford, A rapid and sensitive method for the quantitation microgram quantities of a protein isolated from red cell membranes, Anal Biochem. 72 (1976) 248–254, https://doi.org/10.1016/0003-2697(76)90527-3.

[28] M. Dubois, K. Gilles, J. Hamilton, P. Rebers, F. Smith, Phenol sulphuric acid method for total carbohydrate, Anal. Chem. 26 (1956) 350–356, https://doi.org/10.1021/ac60111a017.
[29] R. Campo, S. Sguanci, S. Caffaz, L. Mazzoli, M. Ramazzotti, C. Lubello, T. Lotti, Efficient carbon, nitrogen and phosphorus removal from low C/N real domestic wastewater with aerobic granular sludge, Bioresour. Technol. 305 (2020) 122961, https://doi.org/10.1016/j.biortech.2020.122961.
[30] M. Kreuk, M.V. Loosdrecht, Selection of slow growing organisms as a means for improving aerobic granular sludge stability, Water Sci. Technol. 49 (2004) 9, https://doi.org/10.2166/wst.2004.0792.
[31] D. Wu, Z. Zhang, Z. Yu, L. Zhu, Optimization of F/M ratio for stability of aerobic granular process via quantitative sludge discharge, Bioresour. Technol. 252 (2018) 150–156, https://doi.org/10.1016/j.biortech.2017.12.094.
[32] R.A. Hamza, Z. Sheng, O.T. Iorhemen, M.S. Zaghloul, J.H. Tay, Impact of food-to-microorganisms ratio on the stability of aerobic granular sludge treating high-strength organic wastewater, Water Res. 147 (2018) 287–298, https://doi.org/10.1016/j.watres.2018.09.061.
[33] R.A. Hamza, O.T. Iorhemen, M.S. Zaghloul, J.H. Tay, Rapid formation and characterization of aerobic granules in pilot-scale sequential batch reactor for high-strength organic wastewater treatment, J. Water Process. Eng. 22 (2018) 27–33, https://doi.org/10.1016/j.jwpe.2018.01.002.
[34] B.S. Mcswain, R.L. Irvine, P.A. Wilderer, The influence of settling time on the formation of aerobic granules, Water Sci. Technol. 50 (2004) 195–202, https://doi.org/10.2166/wst.2004.0643.
[35] A. Jafari Kang, Q. Yuan, Long-term stability and nutrient removal efficiency of aerobic granules at low organic loads, Bioresour. Technol. 234 (2017) 336–342, https://doi.org/10.1016/j.biortech.2017.03.057.
[36] M. Verawaty, M. Pijuan, Z. Yuan, P.L. Bond, Determining the mechanisms for aerobic granulation from mixed seed of floccular and crushed granules in activated sludge wastewater treatment, Water Res. 46 (2012) 761–771, https://doi.org/10.1016/j.watres.2011.11.054.
[37] M. Von Sperling, Activated sludge and aerobic biofilm reactors, Water Intell. 6 (0) (2007), https://doi.org/10.2166/9781780402123.
[38] J.J. Beun, K. Dircks, M.C.M. Van Loosdrecht, J.J. Heijnen, Poly-b-hydroxybutyrate metabolism in dynamically fed mixed microbial cultures, Water Res. 36 (2002) 1167–1180, https://doi.org/10.1016/S0043-1354(01)00317-7.
[39] L. Qin, L. Liu, Z. Wang, W. Chen, D. Wei, Efficient resource recycling from liquid digestate by microalgae-yeast mixed culture and the assessment of key gene transcription related to nitrogen assimilation in microalgae, Bioresour. Technol. 264 (2018) 90–97, https://doi.org/10.1016/j.biortech.2018.05.061.
[40] S. Jia, S. Wang, J. Zhao, X. Li, Q. Zhang, Y. Peng, Effect of endogenous denitrification rate of domesticated GAOs on NO2–N and NO3–N, CIES J. 68 (2017) 4731–4738, https://doi.org/10.11949/j.issn.0438-1157.20170734.
[41] J. Zhao, X. Wang, X. Li, S. Jia, Q. Wang, Y. Peng, Improvement of partial nitrification endogenous denitrification and phosphorus removal system: balancing competition between phosphorus and glycogen accumulating organisms to enhance nitrogen removal without initiating phosphorus removal deterioration, Bioresour. Technol. 281 (2019) 382–391, https://doi.org/10.1016/j.biortech.2019.02.109.
[42] M. Layer, A. Adler, E. Reynaert, A. Hernandez, M. Pagni, E. Morgenroth, C. Holliger, N. Derlon, Organic substrate diffusibility governs microbial community composition, nutrient removal performance and kinetics of granulation of aerobic granular sludge, Water Res. X 4 (2019), 100033, https://doi.org/10.1016/j.wroa.2019.100033.
[43] W. Zhang, X. Dai, B. Dong, L. Dai, New insights into the effect of sludge proteins on the hydrophilic/hydrophobic properties that improve sludge dewaterability during anaerobic digestion, Water Res. 173 (2020), 115503, https://doi.org/10.1016/j.watres.2020.115503.
[44] X. Ran, L. Lin, M. Ying, A label-free proteomic approach differentiates between conventional and organic rice, J Food Compos Anal. 80 (2019) 51–61, https://doi.org/10.1016/j.jfca.2019.04.004.
[45] M. Ashburner, C.A. Ball, J.A. Blake, D. Botstein, H. Butler, J.M. Cherry, A.P. Davis, K. Dolinski, S.S. Dwight, J.T. Eppig, M.A. Harris, D.P. Hill, L. Issel-Tarver, A. Kasarskis, S. Lewis, J.C. Matese, J.E. Richardson, M. Ringwald, G.M. Rubin, G. Sherlock, Gene ontology: tool for the unification of biology, Nat Genet. 25 (1) (2000) 25–29, https://doi.org/10.1038/75556.
[46] C.-Y. Xing, T.-F. Ma, J.-S. Guo, Y. Shen, P. Yan, F. Fang, Y.-P. Chen, Bacterially self-assembled encapsulin nanocompartment for removing silver from water, Water Res. 191 (2021), 116800, https://doi.org/10.1016/j.watres.2020.116800.
[47] W.-M. Li, X.-W. Liao, J.-S. Gio, Y.-X. Zhang, Y.-P. Chen, F. Fang, P. Yan, New insights into filamentous sludge bulking: the potential role of extracellular polymeric substances in sludge bulking in the activated sludge process, Chemosphere 248 (2020), 126012, https://doi.org/10.1016/j.chemosphere.2020.126012.
[48] R.D. Franca, H.M. Pinheiro, M.C. van Loosdrecht, N.D. Lourenço, Stability of aerobic granules during long-term bioreactor operation, Biotechnol. Adv. 36 (2018) 228–246, https://doi.org/10.1016/j.biotechadv.2017.11.005.
[49] Z. Zhang, J. Qiu, R. Xiang, H. Yu, X. Xu, L. Zhu, Organic loading rate (OLR) regulation for enhancement of aerobic sludge granulation: role of key microorganism and their function, Sci. Total Environ. 653 (2019) 630–637, https://doi.org/10.1016/j.scitotenv.2018.10.418.
[50] Y. Feng, Y. Zhao, Y. Guo, S. Liu, Microbial transcript and metabolome analysis uncover discrepant metabolic pathways in autotrophic and mixotrophic anammox consortia, Water Res. 128 (2018) 402–411, https://doi.org/10.1016/j.watres.2017.10.069.
[51] Chenyang Ma, Wei Zeng, Qingan Meng, Chunyan Wang, Y. Peng, Identification of partial denitrification granulation enhanced by low C/N ratio in the aspect of metabolomics and quorum sensing, Chemosphere. 286 (2022) 131895. doi: 10.1016/j.chemosphere.2021.131895.
[52] A.M.S. Paulo, C.L. Amorim, J. Costa, D.P. Mesquita, E.C. Ferreira, P.M.L. Castro, Long-term stability of a non-adapted aerobic granular sludge process treating fish canning wastewater associated to EPS producers in the core microbiome, Sci. Total Environ. 756 (2021), 144007, https://doi.org/10.1016/j.scitotenv.2020.144007.
[53] A.S. Oliveira, C.L. Amorim, D.P. Mesquita, E.C. Ferreira, M. van Loosdrecht, P.M. L. Castro, Increased extracellular polymeric substances production contributes for the robustness of aerobic granular sludge during long-term intermittent exposure to 2-fluorophenol in saline wastewater, J. Water Process. Eng. 40 (2021), 101977, https://doi.org/10.1016/j.jwpe.2021.101977.
[54] G.-P. Sheng, M.-L. Zhang, H.-Q. Yu, Characterization of adsorption properties of extracellular polymeric substances (EPS) extracted from sludge, Colloid Surface B 62 (2008) 83–90, https://doi.org/10.1016/j.colsurfb.2007.09.024.
[55] W. Yin, Y. Wang, L. Liu, J. He, Biofilms: the microbial “protective clothing” in extreme environments, Int. J. Mol. Sci. 20 (2019) 3423, https://doi.org/10.3390/ijms20143423.
[56] R.J. Zeng, Z. Yuan, J. Keller, Enrichment of denitrifying glycogen-accumulating organisms in anaerobic/anoxic activated sludge system, Biotechnol. Bioeng. 81 (2003) 397–404, https://doi.org/10.1002/bit.10484.